ACS Sustainable Chemistry & Engineering

pubs.acs.org/journal/ascecg

Research Article

Highly Effective Functionalized Coatings with Antibacterial and Antifouling Properties

Marios Michailidis,* Eldad Gutner-Hoch, Reut Wengier, Rob Onderwater, Raechelle A. D'Sa, Yehuda Benayahu, Anton Semenov, Vladimir Vinokurov, and Dmitry G. Shchukin*

Cite This: https://dx.doi.org/10.1021/acssuschemeng.0c00998

Read Online

ACCESS | Metrics & More | Article Recommendations | Supporting Information

ABSTRACT: One of the current challenges in maritime antifouling is the development of new nanostructured coatings which can replace the old protection coatings based on tributyltin biocides prohibited by EU and US legislation as ecologically dangerous. In our study, antibacterial/antifouling polymer coatings containing innovative dual functionalized nanocapsules demonstrate high antifouling activity in various tests. Capsules are MCM-48 SiO_2 nanoparticles loaded with eco-friendly 4,5-dichloro-2-octyl-4-isothiazolin-3-one (DCOIT) antifouling agent and decorated with dimethyloctadecyl [3-(trimethoxysilyl) propyl] ammonium chloride or dimethyltetradecyl [3-(triethoxysilyl) propyl] ammonium chloride (quaternary ammonium salts, QASs) also possessing antifouling activity. Cross section images of the coatings demonstrated the absence of the capsule aggregates in the coatings with slight increase of the surface roughness. The formulated coatings revealed excellent antibacterial performance against *E. coli* and *Staphylococcus aureus* according to ISO 22196:2011 protocol. This antifouling activity was also confirmed by immersion of the coated polyvinyl chloride (PVC) panels at a depth of 8−9 m in the sea (Eilat, Israel). Biofouling coverage of 6.9% was observed for nanocapsules-loaded coatings (5 wt % concentration of nanocapsules) compared to the 49% of the coverage for nonmodified coating after 6 months of immersion. The nanocapsules-loaded coatings with dual antifouling functionality demonstrated antifouling activity even after complete release of encapsulated DCOIT because of chemically attached QAS groups on the nanoparticles surface. Moreover, active antifouling materials presented in nanocapsules do not demonstrate any toxicity to the brine shrimps *Artemia salina*, which are widely used in the food industry.

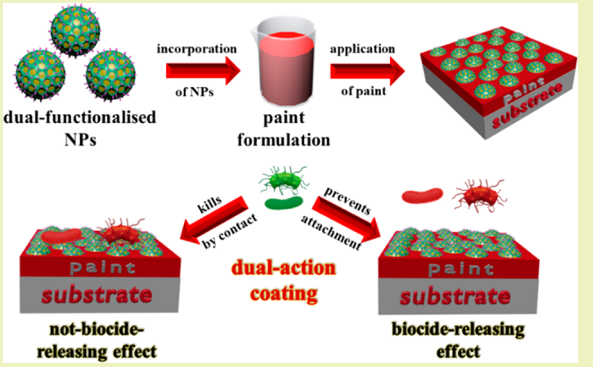

KEYWORDS: *Nanoparticles, Surface modification, Encapsulation, Quaternary ammonium salt, Isothiazolinone*

INTRODUCTION

Biofouling is, actually, a natural corrosion processes resulting in degradation of materials. As any other type of corrosion, it requires a wetted surface (not necessary full immersion in water) and access to the environment.[1] The biofouling process starts from the accumulation of microorganisms or algae on the substrate surface.[1,2] The next stage is the physical adsorption and growth of bacteria, protozoa, and diatoms on the fouled surfaces, so-called microfouling stage. The resulting microbiofilm is a perfect food for larger deposits like spores and invertebrates (soft macrofouling) and, on the last stage, captures mussels, barnacles, and sponges as well as spores.[3−5] Recently, this classic succession mechanism was competed by an alternative dynamic colonisation model where the fouling of the surfaces occurs not from "small to large" organisms.[1] According to this model, different colonies can appear simultaneously because of the great diversity of bioorganisms in water.

This biofouling in maritime applications results in considerable economic and ecological problems. For example, formation of a biofouling film on ship hulls increases the hydrodynamic volume of a vessel and its hydrodynamic friction during the movement through water.[6] Consequently, the maximum speed achievable is decreased leading to 40% increase of fuel consumption. This additional fuel consumption promotes the emission of harmful compounds such as CO_2, SO_x and NO_x into the environment.[7] Biofouling is estimated to cost more than US$ 150 billion annually resulting from the cleaning or even replacement of the components of submerged constructions like oil pipelines and platforms, ship hulls, bridges, etc.[7,8] Because the diversity of fouling organisms is vast and the range of adhesion mechanisms is broad, it is very

Received: February 6, 2020
Revised: May 31, 2020
Published: June 3, 2020

difficult or even impossible to develop universal antifouling coatings.

Since the 1960s, the most successful antifouling paints contain organotin compounds as antifouling agents, especially tributyltin (TBT). However, the increasing use of such paints resulted in the poisoning and depletion of the fish population, and, especially, bivalves.[9] Therefore, the high toxicity of organotin compounds led to their direct banning by the International Maritime Organisation in 2008.[10]

Therefore, the antifouling paint manufacturers first switched to the established biocides from the past such as copper which is known for its antifouling properties since 300 B.C. from the ancient Greeks and Romans.[11] The current functioning of the most of antifouling paints is based on copper as the main component of tin-free alternative biocidal compounds.[12]

At present, the commercially available antifouling coatings are either biocide-releasing or not-biocide-releasing ones.[4] Each system experiences advantages and disadvantages. For instance, the nonbiocide-released antifouling coatings (or fouling release coatings) prevent the attachment of biofoulants mostly on hydrophobic surfaces by providing a low-friction surface on which the organisms have great difficulty to adhere when the ship is underway because they experience hydrodynamic forces on the ship's hull. These surfaces are good for preventing macrofouling, but suffer from microbial biofilm adhesion.[13] On the other hand, the biocide-releasing coatings are more effective but their antifouling activity is being diminished during their lifetime.[14] Usually, the biocides are simply embedded and dispersed molecularly in the polymer matrix of the coating and the antifouling action becomes short due to premature depletion of the active substance to the surrounding environment. Therefore, an excessive amount of biocides is required in order to maintain the antifouling activity of the coating for a longer period which may pollute the marine environment and harm nontarget species.[15] One method to address this problem is the encapsulation of biocides into the nanocarriers followed by their addition to the paint. This technique was successfully used in the past for drug delivery, in biomedical systems, for protection against corrosion and in energy storage systems.[16−21] Encapsulation of biocides into nanocarriers provides a methodology to decrease and control the release rate of the biocides and, at the same time, protect them from the interaction with coating matrix.[22−25]

During recent years, an increased attention was paid to the development of engineered nanoparticles (ENPs) as potential antifouling inhibitors due to their unique physicochemical properties. Low concentrations of nanoparticles in coating formulations exhibit enhanced properties as compared to conventional microscale fillers in coatings. Enhanced properties include, among others, mechanical and optical characteristics, antibacterial/antifouling activity, and wettability that can be further improved by modifying nanoparticles in the coating formulations.[6,26−28] Most commonly used ENPs for antibacterial and antifouling applications are based on functionalized carbon nanotubes, TiO_2, ZnO, chitosan, and silver nanoparticles.[29−31] However, the use of ENPs based on silica nanoparticles as functional fillers for antibacterial/antifouling coating is not well studied yet, especially silica ENPs with enhanced dual functionalization.

This work is focused on the development of novel nanostructured coatings for antibacterial/antifouling applications. For this purpose, we synthesized dual functionalized mesoporous silica nanoparticles (MSNs) as a functional additive for the coatings.[32] The surface of the MSNs was modified with two different types of quaternary ammonium salts (QASs) having effective antibacterial/antifouling properties.[33] The QASs provide to the MSNs an almost permanent antibacterial/antifouling effect due to the covalent attachment on the surface. Afterward, the QAS-modified MSNs were loaded with a liquid biocide (Parmetol S15) in order to achieve an enhanced dual antibacterial/antifouling effect. The main component of the commercial Parmetol S15 biocide is 4,5-dichloro-2-octyl-4-isothiazolin-3-one (DCOIT). It is a hydrophobic antifouling agent with good biodegradability and low water solubility which was recognized first by the Environmental Protection Agency (EPA) Green Chemistry award in 1996. Previously, release of DCOIT from the coatings was shown for directly incorporated DCOIT.[34] In our paper, we demonstrate prolonged antifouling efficiency of encapsulated DCOIT.

The designed nanoparticles were added in biocide-free paint and applied on polyvinyl chloride (PVC) panels. The nanoparticles were dispersed in the paint. Developed paints showed low toxicity against nontarget species and excellent antibacterial and antifouling properties during a six-month field test trial in Red Sea water. In our work, we demonstrate for the first time antifouling coatings with dual antifouling effect based both on passive protection by QAS-modified silica nanocontainers and active controlled release of low toxic DCOIT biocide. These novel antibacterial/antifouling paints have the potential to be used as an effective alternative to the toxic TBT-loaded paints. Our paints combined two basic approaches of the paint industry (biocide-releasing and not-biocide-releasing ones) in one formulation. The modified MSNs provide dual prolonged antibacterial/antifouling properties due to the existence of the chemically attached QAS groups on the nanoparticles surface (not-biocide-releasing approach) and encapsulated biocide (biocide-releasing approach).

EXPERIMENTAL SECTION

Materials. Tetraethyl orthosilicate (TEOS 98%), hexadecyltrimethylammonium bromide (CTAB 99%), and ethanol (99.8%) were purchased from Sigma-Aldrich. Ammonium hydroxide solution (32%) was purchased from Merck. Dimethyloctadecyl [3-(trimethoxysilyl) propyl] ammonium chloride (QC18 60% in methanol) was purchased from Acros Organics while dimethyltetradecyl [3-(triethoxysilyl) propyl] ammonium chloride (QC14) was synthesized in our laboratory. Parmetol S15 was purchased from Schulke AG. All commercial reagents were used without further purification. Polyvinyl chloride (PVC, DSA100) panels were purchased from Kruss Scientific.

Synthesis of Modified Mesoporous Silica Nanoparticles. A detailed description of the synthesis and characterization of the modified nanoparticles used in this study can be found in our previous work.[32] In brief, spherical mesoporous silica nanoparticles (MCM-48) were synthesized by using the modified Stöber's method.[35] Hexadecyltrimethylammonium bromide (2.6 g) was dissolved in a mixture of deionized water (120 mL) and pure ethanol (50 mL), and ammonium hydroxide (12 mL of 32 wt % solution) was added to the surfactant solution. After stirring for 10 min at 600 rpm, tetraethyl orthosilicate (3.4 g) was added at once. After stirring for 16 h at room temperature, the resulting solid deposit was washed twice with ethanol, washed twice with distilled water, and dried at ambient conditions. The organic template was removed by calcination in atmospheric conditions at 550 °C for 6 h with a ramp of 1 °C/min.

The surface of MCM-48 nanoparticles was modified by two different types of QASs, QC18 and QC14, which possess high

https://dx.doi.org/10.1021/acssuschemeng.0c00998
ACS Sustainable Chem. Eng. XXXX, XXX, XXX−XXX

antifouling efficiency.[33,34] The QAS-modified MCM-48 was prepared by hydrolysis and condensation reactions between the quaternary ammonium salt and hydroxyl groups on the surface of MCM-48. A total of 1 g of calcined MCM-48 powder was dispersed in a mixture of ethanol (50 mL) and deionized water (50 mL) using sonication bath. Then 0.5 mL of either QC18 or QC14 was then added and stirred for 24 h at room temperature. The modified nanoparticles were collected by centrifugation, washed twice with ethanol and twice with water to remove the residual reagents, and dried at ambient conditions.

Then, the loading of Parmetol S15 (DCOIT) was performed under vacuum. Modified MCM-48 nanoparticles were directly dispersed in Parmetol S15 reagent using ultrasonic bath and left overnight under vacuum (Figure S1). Then, loaded nanocontainers were washed with water and dried at room temperature in open air. The loading efficiencies of the biocide were measured by TGA. QC18-modified MCM-48 nanocontainers had 26.9 wt % biocide loading while QC14-modified MCM-48 had 31.5 wt % biocide (see also Figure S2 in the Supporting Information). The differences can be explained by blocking some of the silica pores with long-chain QCs, and in the case of the QC18 modified MSNs, the blockage of the pores is higher due to its larger molecular size resulting in lower biocide loading.

In this work we used four different types of antifouling nanocapsules: QC18/Parmetol S15 MCM-48, QC14/Parmetol S15 MCM-48, QC18/MCM-48, and QC14/MCM-48. The presence of all components of composite nanocontainers was also confirmed by FTIR and elemental analysis (see Figure S3 and Tables S1−S3 in the Supporting Information).

Preparation of Coating Formulations Containing Modified Mesoporous Silica Nanoparticles. Antifouling paints were prepared by mixing antifouling capsules with Jotun paint formulation (Jotaguard) via a homogenizer (Bio-Gen PRO200, Pro Scientific) with either 2 or 5 wt % concentration of antifouling capsules. Four different paint formulations were developed for further testing: Paint 1 with 2 or 5 wt % of QC18/Parmetol S15 MCM-48; paint 2 with 2 or 5 wt % of QC14/Parmetol S15 MCM-48; paint 3 with 2 or 5 wt % QC18/MCM-48; and paint 4 with 2 or 5 wt % QC14/MCM-48. All coatings revealed slightly negative surface charge in contact with seawater.

Physico-Chemical Characterization Methods. Focused ion beam scanning electron microscopy (FIB-SEM) was used to obtain cross-sectional images of the pristine and nanocontainer-doped coating formulations. For the preparation of the samples, small PVC plates (typically 10 mm × 10 mm) coated either with pristine or nanocontainer-doped paints were attached with double-sided carbon tape to SEM stub. Afterward, the samples were coated by gold sputtering prior to the measurement. The measurements were performed with FEI Helios Nanolab 600i dual-beam FIB-SEM.

Surface roughness was measured by two channel grindometer (Ascott Analytical Equipment Limited). We used approximately 3 mL of either pristine or nanocontainer-doped paint. The process was repeated at least 9 times and the results were averaged.

The contact angle measurements were performed with an Attension Theta (Biolin Scientific) contact angle meter interfaced to drop shape analysis software. PVC plates 5 cm × 5 cm were coated with the pristine paint and four nanocontainer-doped paints. We used three coated PVC replicas for each type of paint, and water contact angles were obtained in three different areas for each replica. Afterward, the overall values for each type of the paints were averaged.

FTIR characterization was done using Bruker TENSOR II FTIR spectrometer equipped with diffuse reflectance accessory (EasyDiff, Pike Technologies, Madison, WI, U.S.A.). A small quantity of pristine or modified MCM-48 (approximately 10 wt %) was mixed with KBr using pestle and mortar. After fine grinding, the powder sample was placed in the FTIR microcup. Finely ground KBr was used as a background. All spectra were recorded within the range of 4000−400 cm^{-1} with resolution 4 cm^{-1} and 128 scans and submitted to background spectrum subtraction.

Antibacterial Activity of Coating Formulations Containing Antifouling Capsules. For evaluation of the antibacterial properties of coating formulations, 5 cm × 5 cm PVC plates were coated with the pristine paint and the nanocontainer-doped paints (containing 5 wt % modified nanoparticles) and tested against Gram-positive *Staphylococcus aureus* (*S. aureus*) and Gram-negative *Escherichia coli* (*E. coli*) bacteria according to ISO 22196:2011 protocol (three replicate samples of each paint formulation were tested).[36] First, the *E. coli* (ATCC 10536) and *S. aureus* (ATCC 25923) strains were grown on nutrient broth agar (NB) for 24 h at 37 °C. The test inoculum was prepared by transferring one colony of the test bacteria into a small amount of 1/500 NB, and after serial dilutions, the bacterial concentration was between 2.5×10^5 and 1×10^6 colony forming units per mL (CFU/mL). The coated PVC test specimens were placed in sterile Petri dishes and inoculated by 0.4 mL of the test inoculum. A sterile polypropylene film cover (4 cm × 4 cm) was placed on top of the liquid and the inoculum was spread to its edges. The inoculated specimens were then incubated at 35 °C for 24 h under humid conditions (above 90% humidity). After the incubation, the bacteria remaining on the test specimens and the cover film were completely recovered in 10 mL of the recovery solution. Then, 100 μL of the recovery solution with the surviving test bacteria was added to 100 μL of NB medium in oxygen biosensor 96-well round-bottom microplate containing 50 μL of 2000 ppm tris(bathophenanthroline)-ruthenium(II) chloride adsorbed on pore glass embedded in a PDMS matrix (OBS). A thin film of petroleum oil was placed on top of the liquid to limit oxygen exchange from the air to the liquid. The plate was incubated inside a Becton-Dickinson DTX880 fluorescence microplate reader at 37 °C for 16 h, and the fluorescence (ex: 450 nm, em: 630 nm) of the OBS was measured from the bottom every 10 min. The time-to-threshold (3 times above background) was determined for each sample as compared to the calibration curve of a 10-fold serial dilution of the test bacteria from 1×10^8 to 1×10^1 CFU's of bacteria. The growth of *S. aureus* and *E. coli* was determined according to the following eq (eq 1):

$$\text{bacterial growth}(\%) = \left(1 - \left(\frac{A - B}{A}\right)\right) \times 100 \quad (1)$$

where A is the calculated number of CFU's in the control sample based on the calibration curve (PVC panel covered with pristine paint without any biocides) and B is the number of calculated number of CFU's in the tested sample (PVC panel covered with pristine paint which contains the synthesized modified nanoparticles). Three replicate samples were analyzed for each coating for statistical analysis.

Antifouling Activity of Coating Formulations Immersed into Red Sea (Field Test). In order to evaluate the antifouling performance of the nanocontainer-loaded paints, we carried out a field test trial in northern Red Sea, Eilat, Israel. PVC panels of 7 cm × 10 cm coated with five different types of paints (pristine paint and paints 1−4 containing 5 wt % modified nanoparticles, three samples of each paint formulation for statistical analysis) were immersed in northern Gulf of Aqaba (Israel) for a six months field test in order to achieve a realistic assessment of their antifouling properties. PVC panels coated with paint without antifouling capsules were used as control samples. The coated PVC panels were submerged at a depth of 8−9 m (Supporting Information, Figure S4). The panels were photographed monthly, and the percentage of fouling was determined by using the image analysis software ImageJ.[37]

Antimacrofouling Assay. In order to obtain information for the antimacrofouling activity, tissue culture plates (size 6 wells) were coated with the pristine and the nanocontainer-doped paints containing 5 wt % modified nanoparticles (six samples of each paint formulation for statistics) and tested against the *Brachidontes pharaonis* mussels (~2 cm length; Supporting Information, Figure S5). They were collected at the North Beach of Eilat (29°32′N 34°57′E) and placed in an aerated acclimation aquarium containing filtered seawater (FSW, 0.45 μm) 48 h prior to the experiment. Only mussels that produced byssus threads in the acclimation aquarium were placed in coated culture plates for 72 h, with 12 individuals per treatment. After 72 h, the mussels' attachment was examined under a dissecting microscope and the number of developed byssus threads was counted. Mussels were then transferred to a recovery test with

https://dx.doi.org/10.1021/acssuschemeng.0c00998
ACS Sustainable Chem. Eng. XXXX, XXX, XXX−XXX

untreated plates (containing only FSW, 0.45 μm) for 72 h and then similarly examined for attachment and byssus threads. The antimacrofouling efficacy of the paints was presented as percentage of mussels attached on the coated plates after the 72 h of exposure. Information about the toxicity of the paints against the mussels was obtained from the percentage of mussels attached after 72 h of exposure in recovery test. During the test, ambient temperature, photoperiod (light/dark cycle of 12:12 h), pH (8.18 ± 0.03), and salinity (S = 40.5 ± 0.5) were controlled.[38,39] Six replicate samples were analyzed for each coating for statistical analysis.

Nontarget Toxicity Test. The toxicity of the paints was evaluated by a brine shrimp toxicity assay.[40] Eggs of *Artemia salina* were hatched in aerated seawater at 30 °C for 24−30 h. After hatching, the nauplii were transferred in tissue culture plates (size 6 wells, each containing 10 animals, n = 60) coated with the pristine and the nanocontainer-doped paints and incubated at 24 ± 2 °C for 24 h. The percentage of nauplii mortality (lack of mobility) was then recorded.[41,42] Six replicate samples were analyzed for each coating for statistical analysis.

RESULTS AND DISCUSSION

Coating Formulations: Surface Properties and Distribution of Modified Nanoparticles. The nonaggregated dispersion of the modified nanoparticles inside the coating formulations is very critical for performance of the coating since poor distribution of nanoparticles and big aggregates may undermine its antifouling properties. For this reason, we used focused ion beam scanning electron microscopy in order to obtain cross section images and investigate the dispersion of the different types of nanoparticles inside the pristine paint (Figures 1 and S6 in the Supporting Information). The cross section image for the pristine paint showed the existence of nonhomogeneous separate particles with several sizes within the range of a few hundred nm to 7 μm. The pristine paint mainly consists of the polymeric matrix (binder) but the presence of pigments and different types of additives is essential in order to improve the properties of the paint such as color, viscosity, opacity, etc. Therefore, the variation of particles' size and morphology can be attributed to the different components of the initial coating formulation. Dispersion of the silica nanoparticles can be clearly seen in the filtrated pristine paint (Supporting Information, Figure S1). Further confirmation of the dispersity of the particle additives in the paints was achieved by using a grindometer according to the ISO 1524 protocol (Supporting Information, Figure S7). The fineness of grind for the nanocontainer-treated coatings was between 18 and 22 μm, whereas for the pristine paint was 18 μm.

Figure 2 shows the average roughness values for coated PVC panels. The addition of nanoparticles in the pristine paint increased the surface roughness of the coated plates. The average roughness for the pristine paint is 440 nm, it is between 650 and 700 nm for paints 1 and 2 containing the dual functionalized nanocontainers (QAS-modified nanoparticles loaded with biocide) and between 1000 and 1120 nm for the Paints 3 and 4 containing single functionalized nanocontainers (QAS-modified nanoparticles). It is common that the addition of the extra solid component to pristine coating formulation increases coating roughness. Variation of the roughness values for nanocontainer-doped paints can be explained by different types of nanoparticles in formulations. Paints 3 and 4 contain QAS-functionalized nanoparticles. Paints 1 and 2 contain QAS-modified nanoparticles loaded with additional biocide. Before the encapsulation process, the modified nanoparticles were stirred under sonication in liquid

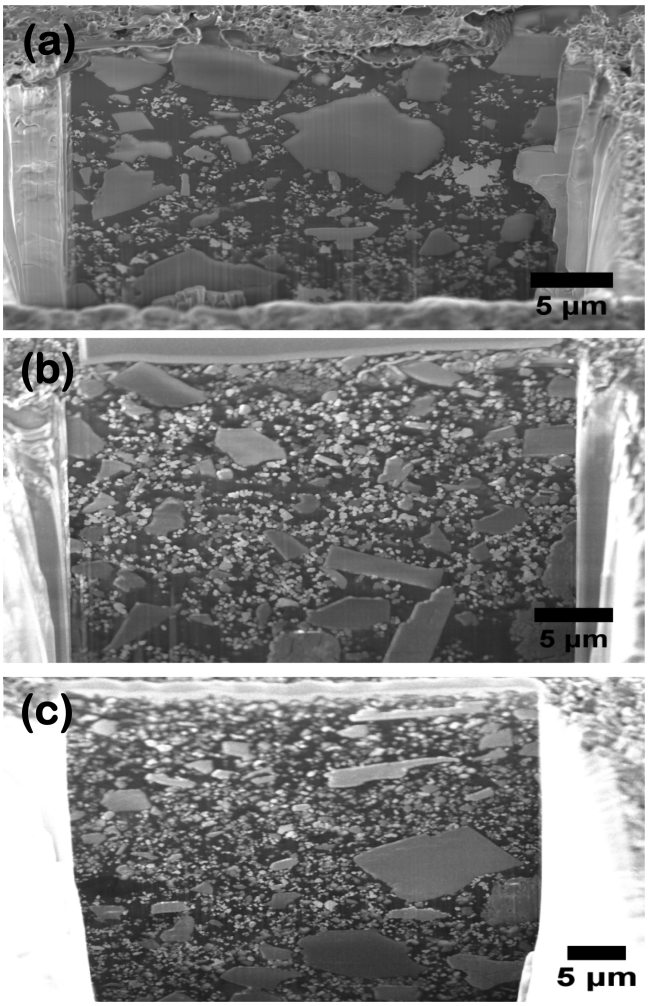

Figure 1. Cross section images (FIB-SEM) for the (a) pristine paint without any modified nanoparticles inside, (b) paint 1, and (c) paint 3.

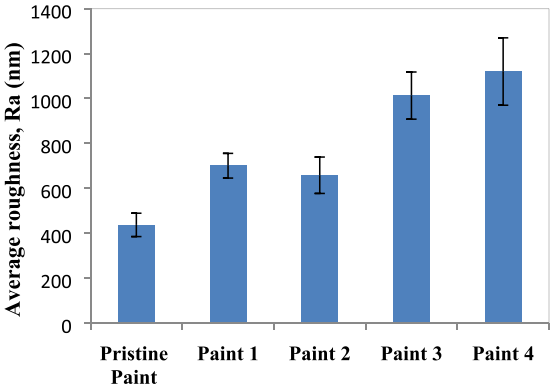

Figure 2. Surface roughness values of PVC panels coated with the pristine paint and paints 1−4 with projected area of 5 mm. Error bars: deviation based on Student distribution for three samples of each paint formulation and three areas for each sample.

biocide for several minutes which decreased the overall surface roughness. The average roughness measurements are consistent with obtained values for the fineness of grind (Supporting Information, Table S4).

Figure 3 illustrates the contact angle values for the coated PVC panels. The pristine paint showed contact angle value of

https://dx.doi.org/10.1021/acssuschemeng.0c00998
ACS Sustainable Chem. Eng. XXXX, XXX, XXX−XXX

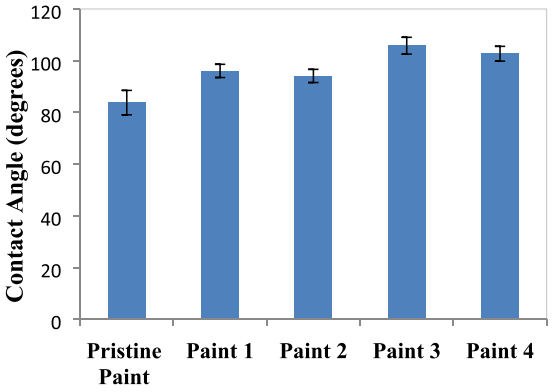

Figure 3. Contact angle values for PVC panels coated with the pristine paint and paints 1−4. Error bars: deviation based on Student distribution for three samples of each paint formulation and three areas for each sample.

84° which is within the hydrophobic region. However, the formulated paints 1−4 displayed contact angle values above 90°. The contact angles for the paints 1−4 (with 5 wt % of modified nanoparticles) were 96°, 94°, 106°, and 103°, respectively (Supporting Information, Figure S8). The addition of modified nanoparticles affected wettability properties of the pristine paint and four nanocontainer-loaded paints exhibited higher hydrophobicity. The increased surface roughness of the nanocontainer-loaded paints compared to pristine paint could be a possible explanation for their increased hydrophobicity.

Antibacterial Performance of PVC Plates Coated with the Nanocontainer-Doped Paints. For evaluation of the antibacterial activity of the nanocontainer-doped paints, 50 mm × 50 mm PVC plates were coated with the pristine paint and paints 1−4 (containing 5 wt % of modified nanoparticles) and tested against Gram negative *Escherichia coli* and Gram positive *Staphylococcus aureus* according to the ISO 22196:2011 protocol. The PVC panels coated with the pristine paint were used as control sample and the number of viable bacteria on these surfaces after 24 h of incubation was defined as 100% growth. Figure 4a illustrates the antibacterial properties of PVC panels coated with paints 1−4 and the pristine paint against *E. coli* bacteria. Paints 3 (containing QC18-modified nanoparticles) and 4 (containing QC14-modified nanoparticles) reduced the number of viable bacteria by 86 and 79% as compared to the pristine paint. Moreover, paints 1 and 2 (containing the QAS-modified Parmitol S15 loaded nanocapsules) demonstrated excellent antibacterial performance against *E. coli* by killing 99% of the bacteria. The results are consistent with our previous studies on the antibacterial properties of the modified nanoparticles in powder form, where the QC18-modified nanoparticles exhibited better antibacterial performance than the QC14-modified nanoparticles and the modified nanoparticles with dual effect killed all of the bacteria at the end of experiments.[32] It is noteworthy to mention that the initial bacterial concentration that was applied on the surfaces coated with the pristine paint for the *E. coli* test was 10^5 CFU/ml but the 100% growth for the control sample (pristine paint) at the end of the experiment corresponded to 10^4 CFU/mL indicating also antibacterial activity of pristine paint. Paints 1 and 2 containing the nanocapsules with the dual functionality showed significantly enhanced performance compared to paints 3 and 4 confirming their synergetic antibacterial effect. The same results were observed for Gram positive *Staphylococcus aureus* (Figure 4b).

Antimacrofouling and Toxicity Assays for Nanocontainer-Doped Paints. The rate of attached mussels on the coated plates after 72 h of exposure is presented in Figure 5 (see also Figure S9, Supporting Information section). About 50% of the mussels were attached on the plates coated with the pristine paint. The QAS-modified nanoparticles (paints 3 and 4) increased the antimacrofouling efficacy of the pristine paint indicating their antifouling properties yielding 33% attachment. The dual functionalized nanoparticles (paints 1 and 2) provided remarkably higher antimacrofouling properties to the pristine paint, and all of the exposed mussels were not able to attach to nanocontainer-doped coatings.

In the recovery test, paints 3 and 4 containing the QAS-modified nanoparticles showed recovery values similar to the pristine paint while paints 1 and 2 containing the dual functionalized nanoparticles exhibited higher recovery values, especially for paint 2 where all of the mussels were able to settle. Therefore, we can assume that nanoparticles added into the paint have nontoxic effect against the mussels and, at the same time, they prevent mussels' attachment. Furthermore, the fact that 50 to 100% of the mussels were able to recover immediately after media replenishment confirms that toxicity of the paints does not cause any irreversible damage to test organisms. The paints consist of several chemical compounds which can be released during the test. Therefore, the mussels

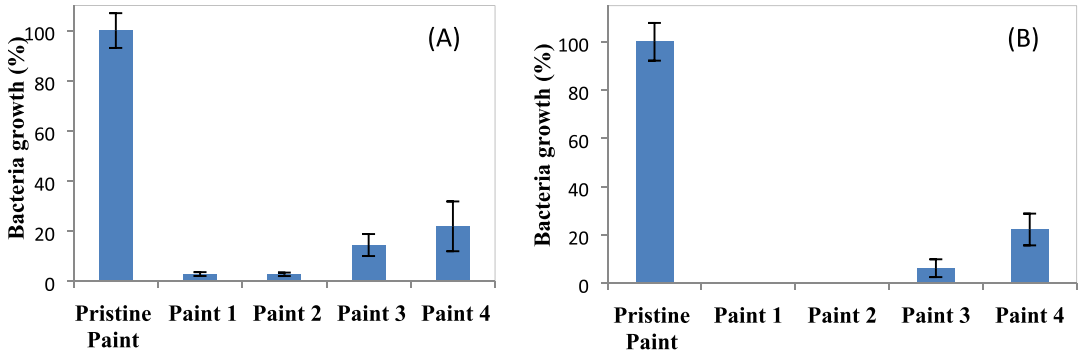

Figure 4. (A) Bacteria growth (*E. coli*) after testing on PVC panels coated with the pristine paint and paints 1−4 by using the ISO 22196:2011 protocol. Error bars: deviation based on Student distribution for three samples of each paint formulation. (B) Bacteria growth (*S. aureus*) after testing on PVC panels coated with the pristine paint and paints 1−4 by using the ISO 22196:2011 protocol. Error bars: deviation based on Student distribution for three samples of each paint formulation.

https://dx.doi.org/10.1021/acssuschemeng.0c00998
ACS Sustainable Chem. Eng. XXXX, XXX, XXX−XXX

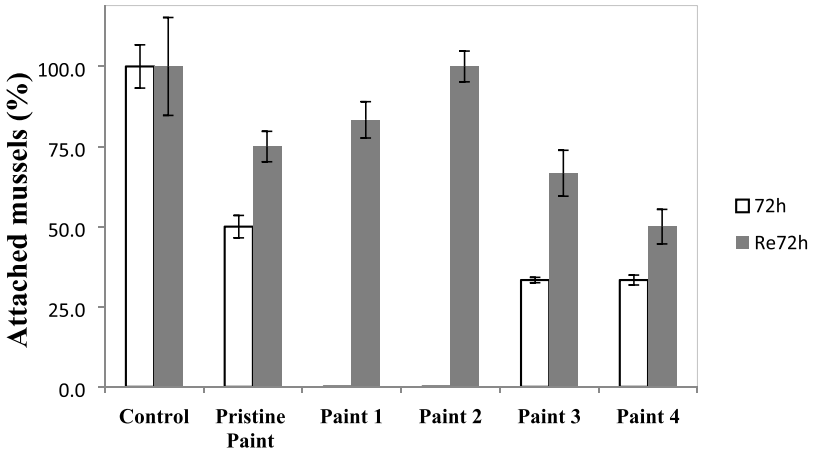

Figure 5. Efficacy antimacrofouling assays of pristine paint and paints 1−4 tested against the Red Sea *Brachidontes pharaonis* mussels indicating number of settled mussels. Blank bars indicate results after 72 h of exposure to treated plates and gray bars after 72 h in recovery assay. Error bars: deviation based on Student distribution for six samples of each paint formulation. Paints 3 and 4 containing the QAS-modified nanoparticles have the same recovery values as pristine paint.

close their shells with increasing concentration of these active compounds as a self-defense mechanism to isolate from the environment.[43]

The *A. salina* nauplii toxicity measurements indicated trends of lethality with paints 1, 3, and 4 showing lower mortality than that of pristine paint (control). Only paint 2 exhibited the trend of slightly higher toxicity than pristine paint (Figure 6).

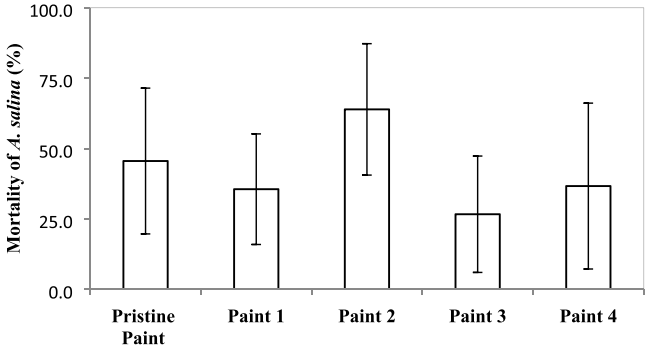

Figure 6. Toxicity assays of pristine paint and paints 1−4 on *Artemia salina* nauplii. Error bars: deviation based on Student distribution for six samples of each paint formulation.

In our previous studies, we found that the amount of the encapsulated biocide in QC14-modified nanoparticles (nanocontainers of paint 2) is slightly higher compared to the biocide encapsulated inside QC18-modified nanoparticles (nanocontainers of paint 1).[32] *A. salina* is filter-feeder and can readily ingest small chemical compounds, even fine particles smaller than 50 μm.[44] Therefore, the higher concentration of biocide in paint 2 could explain its higher toxicity in comparison with paint 1. However, if we take into consideration the statistical errors, we can imply that the toxicity of paints 1−4 falls within the toxicity range of the pristine paint; hence, there is no significant increase in the toxicity of the paints against brine shrimp nauplii by the addition of the four different types of modified nanoparticles, especially for paints 1, 3, and 4.

Antifouling Performance of PVC Panels Coated with the Nanocapsule-Doped Paints. Underwater photographs of the exposed PVC panels coated with the pristine paint and paints 1−4 containing 5 wt % of modified nanoparticles in the first day of immersion and after 6 months in Red Sea are presented in Figure 7. The biofouling coverage on the surface of the control sample coated with the pristine paint was 49% at the end point of this field test. The biofouling coverage of the panels with four nanocapsule-doped Paints was significantly lower, below 10%. Paints 3 and 4 containing the QAS-modified nanoparticles presented 8.6 and 10% of biofouling coverage, respectively. Paints 1 and 2 containing the modified nanocapsules with the dual functionality showed enhanced performance, 6.9 and 8% of biofouling coverage, respectively. Similar tendency was demonstrated in our previous work for 5 months of exposure.[32] However, even after release of all biocide after 5 months of exposure (see DCOIT release profiles in Figure S10, Supporting Information), the covalently attached QAS groups on the surface of nanoparticles continue to provide antifouling properties to the coating formulations prolonging their lifetime antifouling performance, as can be seen for 6 months of exposure.

Figure 8 presents photographs of exposed PVC panels coated with the pristine paint and paints 1−4 containing 2 wt % of modified nanoparticles in the first day of deployment and after 6 months of exposure in Red Sea. Even after decreasing the concentration of the nanoparticles in the coating formulation from 5 to 2 wt %, the paints 1−4 exhibited notably lower biofouling coverage at the end of the 6 months field test trial. In particular, the biofouling coverage after six months of exposure in the Red Sea for the pristine paint was 49%, whereas the paints 1−4 presented 7.5%, 13.9%, 10.5%, and 17.4% of biofouling coverage, respectively.

At the end of the 6 months field test trial, the biofouling coverage on the surfaces of the coated PVC panels with 2 wt % nanoparticles concentration is consistent with biofouling coverage on the surfaces of the coated PVC panels with 5 wt % concentration. Similarly, paints 1 and 2 containing the QAS-modified nanocapsules with the additional encapsulated biocide exhibited higher antifouling properties compared to paints 3 and 4 containing the counterpart nanoparticles with the single functionalization. However, the antifouling performance of the Paints 1−4 was decreased by reducing the amount of the incorporated nanoparticles from 5 to 2 wt %. Furthermore, the antifouling performance of paint 1 compared

https://dx.doi.org/10.1021/acssuschemeng.0c00998
ACS Sustainable Chem. Eng. XXXX, XXX, XXX−XXX

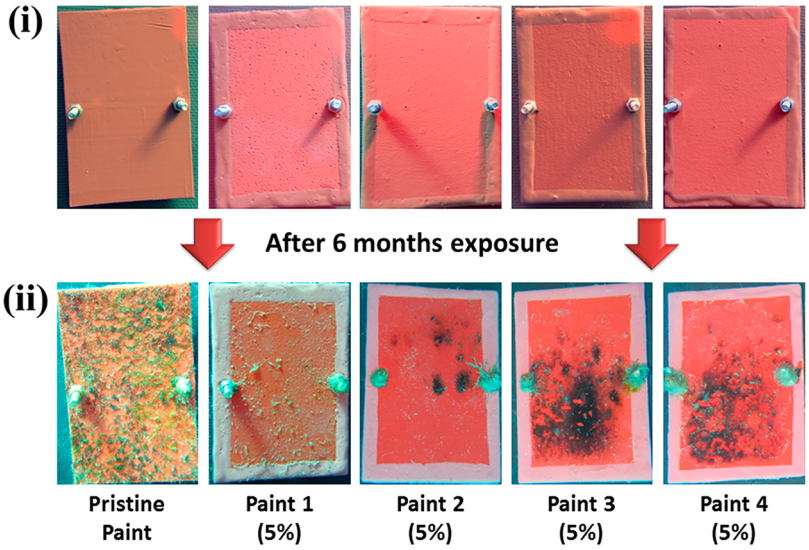

Figure 7. Underwater photographs of PVC panels during the field test trial (Eilat, northern Red Sea) for the first day of deployment (i) and after 6 months of exposure (ii). The PVC panels were coated with five different paints: pristine paint and paints 1−4.

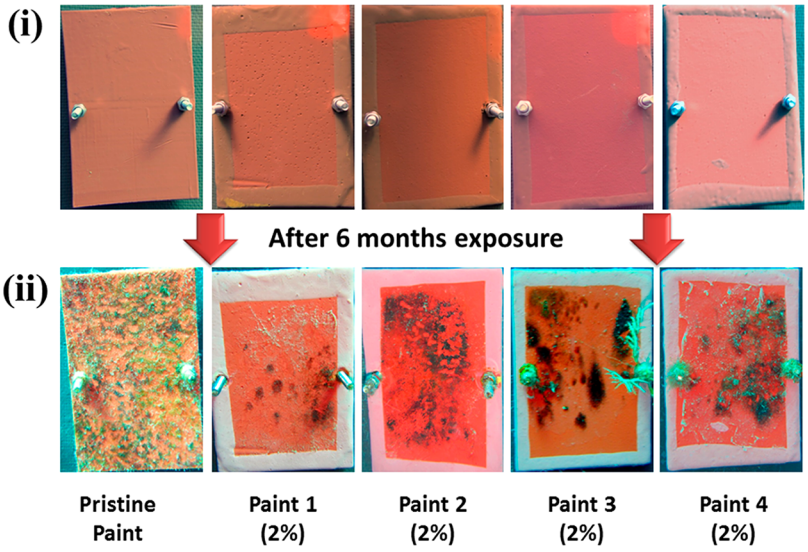

Figure 8. Underwater photographs of PVC panels during the field test trial (Eilat, northern Red Sea) for the first day of deployment (i) and after 6 months of exposure (ii). The PVC panels were coated with five different paints: pristine paint and paints 1−4 containing 2% of active antifouling nanocapsules.

to paint 2 and of paint 3 compared to paint 4 was higher using either 2 or 5 wt % modified nanoparticles. Paints 1 and 3 contain nanoparticles that are surface modified with the quaternary ammonium salt QC18, whereas the nanoparticles for paints 2 and 4 are surface modified with QC14. The main difference between them is that the QC18 has 18 carbons alkyl chain length while the QC14 has 14 carbons alkyl chain length. Therefore, we can assume that the QC18 compound has superior antifouling properties comparing to the QC14 compound, especially in low concentrations in the coating formulation.

Figure 9 illustrates the visual appearance of PVC panels coated with the pristine paint and the two paints with the best performance (paint 1 containing 2 and 5 wt % QC18-modified nanoparticles loaded with biocide) for the first day of deployment and every month of exposure during the 6 months field test trial (see also Figures S11−S12 for additional data, Supporting Information). During the first three months of exposure, the control coating and the two experimental coatings showed qualitatively similar accumulation of biofouling. After longer exposure duration, the effect of the incorporated dual functionalized nanoparticles in the paints can be observed more clearly. In particular, between the four and six months of exposure in the Red Sea, the biofouling accumulation for the pristine paint increased significantly as compared to the two nanocontainer-loaded paints and reached 49% coverage (Figure 9, A4−A6 panels). On the other hand, the biofouling accumulation for paint 1 containing 2 and 5 wt % dual functionalized nanoparticles increased slowly and after 6 months of exposure the coverage was 6.9% for paint 1 with 5% concentration (Figure 9, B6 panel) and 7.5% for paint 1 with 2% concentration (Figure 9, C6 panel).

The antifouling activity of the functionalized coatings derives from both passive and active effects. The effect is passive for the coatings impregnated only with QAS modified silica nanoparticles and is more pronounced for imethylocta-

https://dx.doi.org/10.1021/acssuschemeng.0c00998
ACS Sustainable Chem. Eng. XXXX, XXX, XXX−XXX

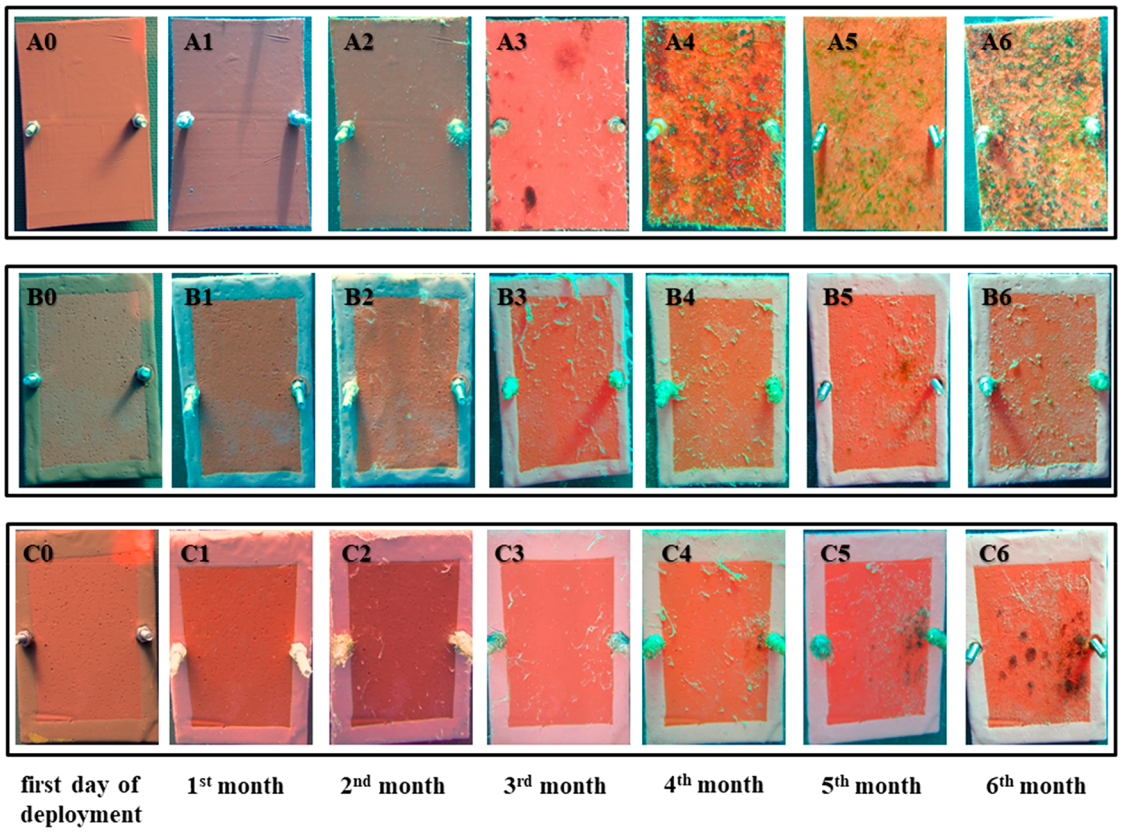

Figure 9. Underwater photographs of PVC panels during the field test trial (Eilat, northern Red Sea) for the first day of deployment and every month of exposure during the six months period. The PVC panels were coated with the pristine paint and the two modified paints with the best performance: (A) pristine paint, (B) paint 1 with 5 wt % of QC18/Parmetol S15 MCM-48 nanocapsules, and (C) paint 1 with 2 wt % QC18/Parmetol S15 MCM-48 nanocapsules.

decyl [3-(trimethoxysilyl) propyl] ammonium chloride QAS with 18 carbon chain than for dimethyltetradecyl [3-(triethoxysilyl) propyl] ammonium chloride with 14 carbon chain. This can be explained by higher penetration level of longer carbon chain into bacteria membrane.

Addition of the encapsulated biocide for active effect considerably increases antifouling activity due to the biocide release. Surprisingly, coating with nanocontainers having lower biocide content (26.9 wt %, paint 1: QC18/Parmetol S15 MCM-48) is more active than paint 2 (QC14/Parmetol S15 MCM-48) with higher biocide content of 31.5 wt %. This allows one to conclude possible synergetic mechanism of the dual functioning antifouling coatings, which involves joint antifouling activity of both QAS with longer chain length (more effective than QAS with shorter chain length) and released biocide. So, one should not describe antifouling properties in a separate manner but as a tandem of two mechanisms. Another important property of the developed coatings is the continuous antifouling activity even after depletion of the encapsulated biocide.

CONCLUSIONS

Among the paints, the best antifouling performance was achieved for paint 1 containing either 2 or 5 wt % of QC18-modified nanoparticles loaded with DCOIT biocide. Furthermore, the QC18-modified nanoparticles provided better antifouling properties to the coating formulations compared to the QC14-modified nanoparticles.

Through our approach, we demonstrated for the first time a facile and effective formulation of antibacterial/antifouling paints containing innovative nanoparticles with dual functionalities in one pot. The combination of the surface modification of mesoporous silica carriers by impregnation with conventional green biocide provides both passive (due to the covalently attached QAS) and active (due to the release of the encapsulated biocide) antifouling protection for current commercially available coatings. The covalently attached QASs on the surface of the nanoparticles remain active even after complete release of the biocide, which considerably increases functional lifetime of nanocapsules-based antifouling coatings.

ASSOCIATED CONTENT

Supporting Information

The Supporting Information is available free of charge at https://pubs.acs.org/doi/10.1021/acssuschemeng.0c00998.

Additional information about the floating underwater platform with the experimental panels for the field tests, images of the tissue culture plates coated with paint for antimacrofouling tests and Red Sea *Brachidontes pharaonis* mussels adhesion, cross section images of the coated PVC panels, two channel grindometer used for the particle size distribution of the paints, contact angle images for water droplets on coated PVC panels, underwater photographs of PVC panels during the field test trial, fineness gauge values for the developed paints, FTIR spectra, ζ-potential measurements, DCOIT release profiles, elemental analysis, and TGA curves for the

https://dx.doi.org/10.1021/acssuschemeng.0c00998
ACS Sustainable Chem. Eng. XXXX, XXX, XXX−XXX

pristine and QAS-modified nanoparticles used in the paint formulations (PDF)

AUTHOR INFORMATION

Corresponding Authors

Marios Michailidis − *Stephenson Institute for Renewable Energy, Department of Chemistry, University of Liverpool, L69 7ZD Liverpool, United Kingdom;* orcid.org/0000-0001-8845-2375; Email: michailidismar@gmail.com

Dmitry G. Shchukin − *Stephenson Institute for Renewable Energy, Department of Chemistry, University of Liverpool, L69 7ZD Liverpool, United Kingdom; Gubkin University, 19991 Moscow, Russia;* orcid.org/0000-0002-2936-804X; Email: D.Shchukin@liverpool.ac.uk

Authors

Eldad Gutner-Hoch − *School of Zoology, George S. Wise Faculty of Life Sciences, Tel Aviv University, 69978 Tel Aviv, Israel; Interuniversity Institute for Marine Sciences in Eilat, Coral Beach 88103, Eilat, Israel*

Reut Wengier − *School of Zoology, George S. Wise Faculty of Life Sciences, Tel Aviv University, 69978 Tel Aviv, Israel*

Rob Onderwater − *Biotech Department, Materia Nova ASBL, B-7822 Ghislenghien, Belgium*

Raechelle A. D'Sa − *Department of Mechanical, Materials and Aerospace Engineering, The Quadrangle, University of Liverpool, L69 3GH Liverpool, United Kingdom;* orcid.org/0000-0003-2651-8783

Yehuda Benayahu − *School of Zoology, George S. Wise Faculty of Life Sciences, Tel Aviv University, 69978 Tel Aviv, Israel*

Anton Semenov − *Gubkin University, 19991 Moscow, Russia;* orcid.org/0000-0003-0660-6233

Vladimir Vinokurov − *Gubkin University, 19991 Moscow, Russia*

Complete contact information is available at: https://pubs.acs.org/10.1021/acssuschemeng.0c00998

Notes

The authors declare no competing financial interest.

ACKNOWLEDGMENTS

This work was financially supported by Russian Science Foundation (Grant 19-79-30091) for development of biocide-loaded nanocontainers. We thank the Interuniversity Institute for Marine Sciences in Eilat (IUI) for assistance and use of facilities. We acknowledge N. Landercy for help with the antibacterial tests. This research was in part supported by the Israel Cohen Chair in Environmental Zoology to Y.B. The field test complied with a permit issued by the Israel Nature and National Parks Protection Authority.

REFERENCES

(1) Callow, J. A.; Callow, M. E. Trends in the Development of Environmentally Friendly Fouling-Resistant Marine Coatings. *Nat. Commun.* **2011**, *2*, 244.

(2) Callow, M. E.; Callow, J. A. Marine Biofouling: A Sticky Problem. *Biologist.* **2002**, *1*, 10−14.

(3) Lejars, M.; Margaillan, A.; Bressy, C. Fouling Release Coatings: A Nontoxic Alternative to Biocidal Antifouling Coatings. *Chem. Rev.* **2012**, *112*, 4347−4390.

(4) Nurioglu, A. G.; Esteves, A. C. C.; de With, G. Non-Toxic, Non-Biocide-Release Antifouling Coatings Based on Molecular Structure Design for Marine Applications. *J. Mater. Chem. B* **2015**, *3*, 6547−6570.

(5) Chambers, L. D.; Stokes, K. R.; Walsh, F. C.; Wood, R. J. K. Modern Approaches to Marine Antifouling Coatings. *Surf. Coat. Technol.* **2006**, *201*, 3642−3652.

(6) Selim, M. S.; Shenashen, M. A.; El-Safty, S. A.; Higazy, S. A.; Selim, M. M.; Isago, H.; Elmarakbi, A. Recent Progress in Marine Foul-Release Polymeric Nanocomposite Coatings. *Prog. Mater. Sci.* **2017**, *87*, 1−32.

(7) Schultz, M. P.; Bendick, J. A.; Holm, E. R.; Hertel, W. M. Economic Impact of Biofouling on a Naval Surface Ship. *Biofouling* **2011**, *27*, 87−98.

(8) Fitridge, I.; Dempster, T.; Guenther, J.; de Nys, R. The Impact and Control of Biofouling in Marine Aquaculture: A Review. *Biofouling* **2012**, *28*, 649−669.

(9) Walmsley, S. Tributyltin Pollution on a Global Scale. An Overview of Relevant and Recent Research: Impacts and Issues. *WWF-UK*, 2006, http://assets.wwf.no/downloads/tbt_global_review_wwf_uk_oct_2006.pdf, accessed 02/06/2020.

(10) IMO. Focus on IMO: Anti-Fouling Systems. *Int. Marit. Organ.* **2002**, *44*, 1−31.

(11) Yebra, D. M.; Kiil, S.; Dam-Johansen, K. Antifouling Technology - Past, Present and Future Steps towards Efficient and Environmentally Friendly Antifouling Coatings. *Prog. Org. Coat.* **2004**, *50*, 75−104.

(12) Omae, I. General Aspects of Tin-Free Antifouling Paints. *Chem. Rev.* **2003**, *103*, 3431−3448.

(13) Molino, P. J.; Childs, S.; Eason-Hubbard, M. R.; Carey, J. M.; Burgman, M. A.; Wetherbee, R. Development of the Primary Bacterial Microfouling Layer on Antifouling and Fouling Release Coatings in Temperate and Tropical Environments in Eastern Australia. *Biofouling* **2009**, *25*, 149−162.

(14) Knowles, B. R.; Wagner, P.; Maclaughlin, S.; Higgins, M. J.; Molino, P. J. Silica Nanoparticles Functionalized with Zwitterionic Sulfobetaine Siloxane for Application as a Versatile Antifouling Coating System. *ACS Appl. Mater. Interfaces* **2017**, *9*, 18584−18594.

(15) Andersson Trojer, M.; Nordstierna, L.; Bergek, J.; Blanck, H.; Holmberg, K.; Nydén, M. Use of Microcapsules as Controlled Release Devices for Coatings. *Adv. Colloid Interface Sci.* **2015**, *222*, 18−43.

(16) Borisova, D.; Möhwald, H.; Shchukin, D. G. Mesoporous Silica Nanoparticles for Active Corrosion Protection. *ACS Nano* **2011**, *5*, 1939−1946.

(17) Graham, M.; Coca-Clemente, J. A.; Shchukina, E.; Shchukin, D. Nanoencapsulated Crystallohydrate Mixtures for Advanced Thermal Energy Storage. *J. Mater. Chem. A* **2017**, *5*, 13683−13691.

(18) Gao, H.; Goriacheva, O. A.; Tarakina, N. V.; Sukhorukov, G. B. Intracellularly Biodegradable Polyelectrolyte/Silica Composite Microcapsules as Carriers for Small Molecules. *ACS Appl. Mater. Interfaces* **2016**, *8*, 9651−9661.

(19) Zheng, Z.; Chang, Z.; Xu, G.-K.; McBride, F.; Ho, A.; Zhuola, Z.; Michailidis, M.; Li, W.; Raval, R.; Akhtar, R.; et al. Microencapsulated Phase Change Materials in Solar-Thermal Conversion Systems: Understanding Geometry-Dependent Heating Efficiency and System Reliability. *ACS Nano* **2017**, *11*, 721−729.

(20) Gao, H.; Wen, D.; Sukhorukov, G. B. Composite Silica Nanoparticle/Polyelectrolyte Microcapsules with Reduced Permeability and Enhanced Ultrasound Sensitivity. *J. Mater. Chem. B* **2015**, *3*, 1888−1897.

(21) Andreeva, D. V.; Fix, D.; Möhwald, H.; Shchukin, D. G. Buffering Polyelectrolyte Multilayers for Active Corrosion Protection. *J. Mater. Chem.* **2008**, *18*, 1738.

(22) Sørensen, G.; Nielsen, A. L.; Pedersen, M. M.; Poulsen, S.; Nissen, H.; Poulsen, M.; Nygaard, S. D. Controlled Release of Biocide from Silica Microparticles in Wood Paint. *Prog. Org. Coat.* **2010**, *68*, 299−306.

(23) Yang, M.; Gu, L.; Yang, B.; Wang, L.; Sun, Z.; Zheng, J.; Zhang, J.; Hou, J.; Lin, C. Antifouling Composites with Self-Adaptive Controlled Release Based on an Active Compound Intercalated into Layered Double Hydroxides. *Appl. Surf. Sci.* **2017**, *426*, 185−193.

https://dx.doi.org/10.1021/acssuschemeng.0c00998
ACS Sustainable Chem. Eng. XXXX, XXX, XXX−XXX

(24) Maia, F.; Silva, A. P.; Fernandes, S.; Cunha, A.; Almeida, A.; Tedim, J.; Zheludkevich, M. L.; Ferreira, M. G. S. Incorporation of Biocides in Nanocapsules for Protective Coatings Used in Maritime Applications. *Chem. Eng. J.* **2015**, *270*, 150−157.
(25) Lamaka, S. V.; Shchukin, D. G.; Andreeva, D. V.; Zheludkevich, M. L.; Möhwald, H.; Ferreira, M. G. S. Sol-Gel/Polyelectrolyte Active Corrosion Protection System. *Adv. Funct. Mater.* **2008**, *18*, 3137−3147.
(26) Wouters, M.; Rentrop, C.; Willemsen, P. Surface Structuring and Coating Performance. *Prog. Org. Coat.* **2010**, *68*, 4−11.
(27) Mallakpour, S.; Khadem, E. Recent Development in the Synthesis of Polymer Nanocomposites Based on Nano-Alumina. *Prog. Polym. Sci.* **2015**, *51*, 74−93.
(28) Lvov, Y.; Abdullayev, E. Functional Polymer-Clay Nanotube Composites with Sustained Release of Chemical Agents. *Prog. Polym. Sci.* **2013**, *38*, 1690−1719.
(29) Jhaveri, J. H.; Murthy, Z. V. P. A Comprehensive Review on Anti-Fouling Nanocomposite Membranes for Pressure Driven Membrane Separation Processes. *Desalination* **2016**, *379*, 137−154.
(30) Li, Q.; Mahendra, S.; Lyon, D. Y.; Brunet, L.; Liga, M. V.; Li, D.; Alvarez, P. J. J. Antimicrobial Nanomaterials for Water Disinfection and Microbial Control: Potential Applications and Implications. *Water Res.* **2008**, *42*, 4591−4602.
(31) Hajipour, M. J.; Fromm, K. M.; Akbar Ashkarran, A.; Jimenez de Aberasturi, D.; Larramendi, I. R. de; Rojo, T.; Serpooshan, V.; Parak, W. J.; Mahmoudi, M. Antibacterial Properties of Nanoparticles. *Trends Biotechnol.* **2012**, *30*, 499−511.
(32) Michailidis, M.; Sorzabal-Bellido, I.; Adamidou, E. A.; Diaz-Fernandez, Y. A.; Aveyard, J.; Wengier, R.; Grigoriev, D.; Raval, R.; Benayahu, Y.; D'Sa, R. A.; et al. Modified Mesoporous Silica Nanoparticles with a Dual Synergetic Antibacterial Effect. *ACS Appl. Mater. Interfaces* **2017**, *9*, 38364−38372.
(33) Tischer, M.; Pradel, G.; Ohlsen, K.; Holzgrabe, U. Quaternary Ammonium Salts and Their Antimicrobial Potential: Targets or Nonspecific Interactions? *ChemMedChem* **2012**, *7*, 22−31.
(34) Dai, G. X.; Xie, Q. Y.; Chen, S. S.; Ma, C. F.; Zhang, G. Z. Biodegradable Poly(ester)-Poly(methyl methacrylate) Copolymer for Marine Anti-Biofouling. *Prog. Org. Coat.* **2018**, *124*, 55−60.
(35) Schumacher, K.; Grün, M.; Unger, K. Novel Synthesis of Spherical MCM-48. *Microporous Mesoporous Mater.* **1999**, *27*, 201−206.
(36) International Organization for Standardization. Measurement of Antibacterial Activity on Plastics and Other Non-Porous Surfaces. ISO 22196, 2011; https://www.iso.org/standard/54431.html, accessed online 02/06/2020.
(37) Schneider, C. A.; Rasband, W. S.; Eliceiri, K. W. NIH Image to ImageJ: 25 Years of Image Analysis. *Nat. Methods* **2012**, *9*, 671−675.
(38) Gutner-Hoch, E.; Martins, R.; Oliveira, T.; Maia, F.; Soares, A.; Loureiro, S.; Piller, C.; Preiss, I.; Weis, M.; Larroze, S.; et al. Antimacrofouling Efficacy of Innovative Inorganic Nanomaterials Loaded with Booster Biocides. *J. Mar. Sci. Eng.* **2018**, *6*, 6.
(39) Figueiredo, J.; Oliveira, T.; Ferreira, V.; Sushkova, A.; Silva, S.; Carneiro, D.; Cardoso, D. N.; Gonçalves, S. F.; Maia, F.; Rocha, C.; et al. Toxicity of Innovative Anti-Fouling Nano-Based Solutions to Marine Species. *Environ. Sci.: Nano* **2019**, *6*, 1418−1429.
(40) Gutner-Hoch, E.; Martins, R.; Maia, F.; Oliveira, T.; Shpigel, M.; Weis, M.; Tedim, J.; Benayahu, Y. Toxicity of Engineered Micro- and Nanomaterials with Antifouling Properties to the Brine Shrimp Artemia Salina and Embryonic Stages of the Sea Urchin Paracentrotus Lividus. *Environ. Pollut.* **2019**, *251*, 530−537.
(41) Solis, P. N.; Wright, C. W.; Anderson, M. M.; Gupta, M. P.; Phillipson, J. D. A Microwell Cytotoxicity Assay Using Artemia Salina (Brine Shrimp). *Planta Med.* **1993**, *59*, 250−252.
(42) Nunes, B. S.; Carvalho, F. D.; Guilhermino, L. M.; Van Stappen, G. Use of the Genus Artemia in Ecotoxicity Testing. *Environ. Pollut.* **2006**, *144*, 453−462.
(43) Wilsanand, V.; Wagh, A. B.; Bapuji, M. Antifouling Activities of Marine Sedentary Invertebrates on Some Macrofoulers. *Indian J. Mar. Sci.* **1999**, *28*, 280−284.
(44) Ates, M.; Daniels, J.; Arslan, Z.; Farah, I. O. Effects of Aqueous Suspensions of Titanium Dioxide Nanoparticles on Artemia Salina: Assessment of Nanoparticle Aggregation, Accumulation, and Toxicity. *Environ. Monit. Assess.* **2013**, *185*, 3339−3348.

https://dx.doi.org/10.1021/acssuschemeng.0c00998
ACS Sustainable Chem. Eng. XXXX, XXX, XXX−XXX